Supplementary Materials: Real-World Vehicle Emission Rate of Particle Size distributions based on Measurement of Tunnel Flow Coefficient

Chaehyeong Park, Myoungki Song, Gyutae Park, Kyunghoon Kim, Taehyoung Lee, Sanguk Lee, Yunsung Lim, Min-Suk Bae

1.Supplementary Information

Table S1. Operating conditions of the two employed the Scanning Mobility Particle Sizers (SMPS).

Type	Condition
1) Electrostatic Classifier 3080	
Aerosol flow	1 L/min
Sheath air	4 L/min
Impactor nozzle size	0.071 cm (d50=670 nm)
Sample size (nm)	11.5 – 604.3
Scan time	300 sec
Channels/Decade	110
2) Long Differential Mobility Analyzer 3081	
3) CPC	
Model	3772
Flow source	External vacuum
Sample flow	1 L/min
Particle counting range	104 particles/cm^3
4) Software	
Aerosol Instrument Manager (AIM)	ver. 9.0.0.0

Operating conditions of the two employed SMPSs are presented in Table S1. The particles, flowing into the ESC via the nozzle of 0.071 cm, are analyzed into 110 channels of particle size distribution from 11.5 nm to 604.3 nm under the condition of flow rate of 1.0 L/min (4.0 L/min. of Sheath Flow). CPC takes particles, separated into each particle size of respective diameters, as condensation nuclei. Particles grow at temperature 22℃ by exploiting the principle of conductive cooling at the state of supersaturation. The analysis of the maximum number concentration of 10,000 N/cm3 from the photometer was enabled by using the laser diode. The Aerosol Instrument Manager (AIM) (ver. 9.0.0.0, TSI Inc., USA) program was used for the calculation of final number concentration.

Table S2. Hourly number concentration discharged from vehicles (ΣN/veh·km) by using the TFC (δ) (m3/veh·km) and hourly number concentrations of particle size distribution inside and outside of the tunnel.

Start time	N/m^3	$m^3/veh{\cdot}km$	$N/veh{\cdot}km$
0	2.44×10^{10}	256	6.96×10^{12}
1	1.9×10^{10}	338	6.65×10^{12}
2	1.92×10^{10}	438	8.53×10^{12}
3	1.95×10^{10}	550	1.25×10^{13}
4	2.65×10^{10}	645	1.97×10^{13}
5	4.00×10^{10}	529	1.64×10^{13}
6	6.01×10^{10}	290	9.05×10^{12}
7	6.07×10^{10}	205	4.81×10^{12}
8	6.02×10^{10}	187	5.29×10^{12}
9	6.72×10^{10}	163	4.85×10^{12}
10	6.24×10^{10}	158	2.93×10^{12}
11	5.46×10^{10}	143	2.26×10^{12}
12	4.72×10^{10}	142	2.97×10^{12}
13	4.04×10^{10}	146	2.68×10^{12}
14	4.87×10^{10}	138	2.20×10^{12}
15	5.20×10^{10}	136	2.38×10^{12}
16	5.58×10^{10}	131	1.70×10^{12}
17	6.83×10^{10}	135	2.34×10^{12}
18	6.56×10^{10}	137	2.40×10^{12}
19	6.05×10^{10}	146	3.17×10^{12}
20	5.17×10^{10}	161	3.52×10^{12}
21	4.06×10^{10}	165	3.06×10^{12}
22	4.35×10^{10}	165	3.88×10^{12}
23	3.03×10^{10}	199	4.91×10^{12}
average	$\mathbf{4.66 \times 10^{10}}$	**238**	$\mathbf{5.63 \times 10^{12}}$

Table S3. Number concentrations of particle size distribution distinguished into values of weekends, weekdays, and period of Asian New Year.

Start time	Weekdays			Weekends			Asian New Year		
	ΔC(N)/m³	m³/veh.km	N /veh.km	ΔC(N)/m³	m³/veh.km	N /veh.km	ΔC(N)/m³	m³/veh.km	N /veh.km
0	2.46×10^{10}	200	4.22×10^{12}	2.67×10^{10}	243	3.41×10^{12}	1.33×10^{10}	318	5.25×10^{12}
1	1.96×10^{10}	267	4.37×10^{12}	2.17×10^{10}	314	3.63×10^{12}	5.60×10^{09}	415	4.23×10^{12}
2	2.02×10^{10}	338	5.65×10^{12}	2.25×10^{10}	423	5.07×10^{12}	7.38×10^{09}	526	5.14×10^{12}
3	2.11×10^{10}	424	7.42×10^{12}	1.86×10^{10}	511	5.45×10^{12}	4.65×10^{09}	672	4.98×10^{12}
4	2.89×10^{10}	459	1.27×10^{13}	2.61×10^{10}	587	9.84×10^{12}	1.08×10^{10}	723	1.18×10^{13}
5	4.53×10^{10}	313	1.89×10^{13}	3.91×10^{10}	550	1.37×10^{13}	1.41×10^{10}	513	1.05×10^{13}
6	7.03×10^{10}	157	1.31×10^{13}	5.46×10^{10}	371	1.25×10^{13}	1.52×10^{10}	357	8.86×10^{12}
7	7.41×10^{10}	113	6.83×10^{12}	4.63×10^{10}	301	8.98×10^{12}	2.06×10^{10}	303	9.53×10^{12}
8	6.87×10^{10}	110	6.75×10^{12}	5.58×10^{10}	260	8.64×10^{12}	2.37×10^{10}	258	9.56×10^{12}
9	7.26×10^{10}	103	6.60×10^{12}	6.75×10^{10}	210	7.71×10^{12}	2.27×10^{10}	206	8.57×10^{12}
10	7.06×10^{10}	105	6.38×10^{12}	6.32×10^{10}	186	7.17×10^{12}	1.82×10^{10}	187	5.43×10^{12}
11	6.03×10^{10}	100	5.11×10^{12}	5.59×10^{10}	174	6.08×10^{12}	2.40×10^{10}	111	4.32×10^{12}
12	5.80×10^{10}	100	5.02×10^{12}	3.89×10^{10}	159	4.55×10^{12}	1.26×10^{10}	118	1.04×10^{12}
13	4.85×10^{10}	106	4.67×10^{12}	3.86×10^{10}	154	4.13×10^{12}	6.56×10^{09}	118	9.35×10^{11}
14	5.54×10^{10}	103	5.03×10^{12}	4.82×10^{10}	143	5.07×10^{12}	5.96×10^{09}	93	8.93×10^{11}
15	6.17×10^{10}	105	5.53×10^{12}	4.11×10^{10}	142	4.52×10^{12}	1.60×10^{10}	90	1.23×10^{12}
16	6.44×10^{10}	101	6.13×10^{12}	5.44×10^{10}	138	4.88×10^{12}	1.73×10^{10}	88	7.47×10^{11}
17	8.16×10^{10}	106	7.40 ×	5.78×10^{10}	149	5.40 ×	1.82×10^{10}	104	8.45 ×

			10^{12}			10^{12}			10^{11}
18	8.04×10^{10}	102	7.59×10^{12}	5.28×10^{10}	157	4.63×10^{12}	1.74×10^{10}	113	1.40×10^{12}
19	7.51×10^{10}	109	6.53×10^{12}	4.67×10^{10}	174	4.68×10^{12}	1.43×10^{10}	122	1.86×10^{12}
20	6.50×10^{10}	123	6.28×10^{12}	3.94×10^{10}	193	4.38×10^{12}	9.07×10^{09}	124	2.01×10^{12}
21	4.77×10^{10}	131	5.05×10^{12}	3.23×10^{10}	182	3.80×10^{12}	1.41×10^{10}	128	2.35×10^{12}
22	5.09×10^{10}	130	5.38×10^{12}	3.66×10^{10}	184	3.86×10^{12}	1.54×10^{10}	138	2.49×10^{12}
23	3.44×10^{10}	158	4.36×10^{12}	3.14×10^{10}	219	3.86×10^{12}	8.29×10^{09}	174	2.36×10^{12}
average	5.41×10^{10}	169	6.96×10^{12}	4.23×10^{10}	255	6.08×10^{12}	1.40×10^{10}	250	4.43×10^{12}

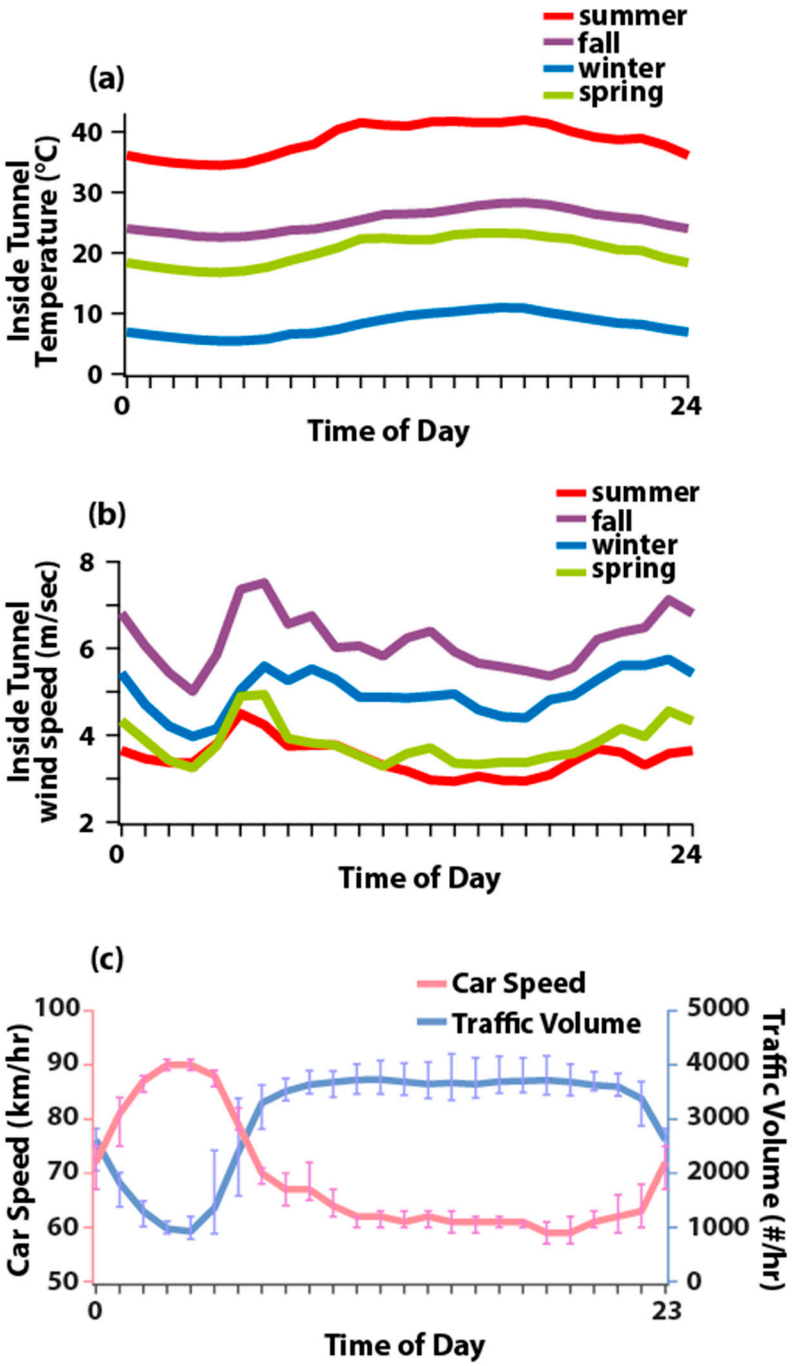

Figure S1. Diurnal patterns of (**a**) temperature, (**b**) wind speed, and (**c**) number of vehicles in season inside of the tunnel to determine the seasonal value of tunnel flow coefficient.

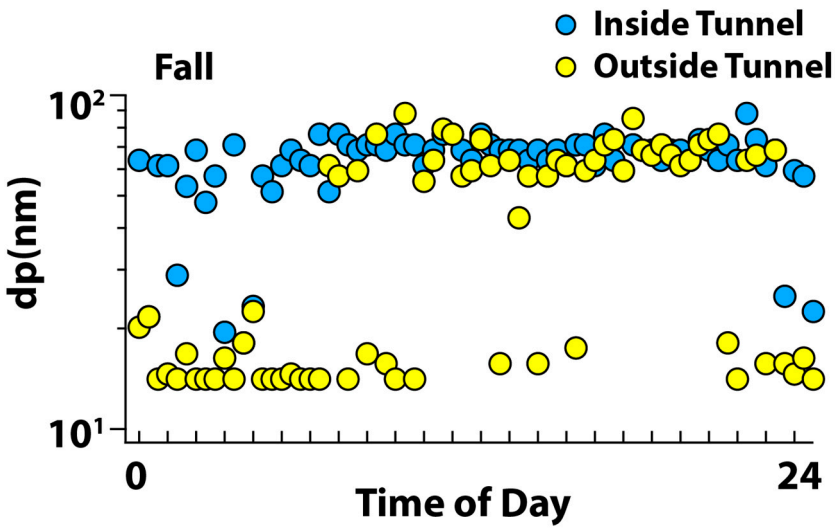

Figure S2. Diurnal pattern of the mode of number concentration of particle size distribution inside and outside of the tunnel employed for the analysis of effects of temperature on the final condensation diameter.